



Article

The Synergistic Effects of SiO₂ Nanoparticles and Organic Photostabilizers for Enhanced Weathering Resistance of Acrylic Polyurethane Coating

Thien Vuong Nguyen ^{1,2,*}, Tuan Anh Nguyen ¹ and Thi Hau Nguyen ³

¹ Institute for Tropical Technology, VAST, 18 Hoang Quoc Viet, Cau Giay, Hanoi 122300, Vietnam; ntanh2007@gmail.com

² Graduate University of Science and Technology, VAST, 18 Hoang Quoc Viet, Cau Giay, Hanoi 122300, Vietnam

³ High School of Education Sciences-University of Education, Viet Nam National University, Kieu Mai street, Bac Tu Liem, Hanoi 143510, Vietnam; haunguyen47@gmail.com

* Correspondence: vuongvast@gmail.com

Received: 28 January 2020; Accepted: 24 February 2020; Published: 26 February 2020



Abstract: This study aims to evaluate the synergical effects of SiO₂ nanoparticles (nano-SiO₂) and organic photostabilizers (Tinuvin 384 (T384) and Tinuvin 292 (T292)) on the weathering resistance of acrylic polyurethane coating. Data obtained from infrared (IR), field emission scanning electron microscopy (FESEM), and weight loss of coatings (before and after aging test), suggest that the SiO₂ nanoparticles play a dual role, as both reinforcer and UV absorber, thus improving effectively both the mechanical properties and the weathering resistance of polyurethane acrylic coatings. The nanocomposite coating containing 2 wt % nano-SiO₂, 2 wt % T384, and 1 wt % T292 exhibits excellent weathering and abrasion resistances, offering a durable outdoor application.

Keywords: acrylic polyurethane coating; nanocomposite; nano-SiO₂; mechanical properties; weathering resistance

1. Introduction

Having many advantages over other conventional polymer coatings, such as good adhesion, transparency, high gloss, and weathering resistance, acrylic polyurethane coating is used widely as a protective and decorative coating for metal structures, interior and exterior wood, and automotive paint [1,2]. Two-component acrylic polyurethane paint can be cured at room temperature through the step-growth polymerization of isocyanate groups with hydroxyl groups in the acrylic polyol resin forming crosslinked urethane.

In order to improve the weathering resistance of the outdoor coatings, in addition to selecting the main components such as resins and pigments with high weathering durability, organic and inorganic light stabilizing additives are usually added to the paint formulation [3–7]. Previous published works showed that organic light stabilizers (such as Tinuvin 384, Tinuvin 1130, Tinuvin 292) exhibited an excellent light stabilizing efficiency. Adding these additives at appropriate content could increase the weathering durability of the polymer coatings by 2–3 times [3]. Besides, as reported in literature, some metal oxides (TiO₂, ZnO, ZrO₂) can absorb ultraviolet (UV) rays, therefore having an ability to protect the polymer substrates from harmful UV light [4–9].

During UV absorption, an electron from the valence band jumps onto the conduction band, leaving a positively charged hole. These electrons and positively charged holes move onto the particle surface, where they recombine to each other or react with oxygen and water to form •OH activated free radicals [4]. These free radicals can be the agent promoting the degradation of polymers. Thus,

metal oxides exhibit the dual effects: (i) Blocking UV rays, and (ii) causing photo-catalytic degradation of the polymer (depending on their content, sizes, structure, and surface modifications) [5].

Currently, the addition of inorganic particles/nanoparticles (at appropriate content) into the polymer substrate can enhance its property [10–16]. Nano-SiO₂ is the most used among the common inorganic nanoparticles. For example, by adding nano-SiO₂ into the coating formulation, the mechanical, thermal, [2,17] weathering resistance [18,19], and anticorrosion properties [20,21] of the organic coatings were significantly improved. Nano-SiO₂ is also used for both super hydrophobic coatings [22–25] or hydrophilic coatings [26].

In our previous work [3], acrylic polyurethane coating with photostabilizers exhibited the lifespan over 12 years under the marine weathering condition (natural exposure). On the other side, as reported in literature, nano-SiO₂ has only been considered as a reinforcer (nanofiller) for polymer matrix. In this study, the combination of nano-SiO₂ and organic light stabilizers (Tinuvin 384, Tinuvin 292) are expected to enhance simultaneously the abrasion resistance and weathering durability of coatings. We will try to explore the role of nano-SiO₂ in this expected enhancement.

2. Experimental

2.1. Materials

The acrylic polyol solution (HSU 1168) obtained from A&P Industrial Resins Company (Taiwan) contained 65 wt % solid, in which the content of hydroxyl groups was 4.3 wt %. The curing agent was polyisocyanate N-75 (75 wt %, Germany) in which the weight percentage of isocyanate groups was 17%. The organic UV absorber, benzotriazole-UV (2-(2-hydroxy-3-tert-butyl-5-propionic acid isooctyl ester)-2H-benzotriazol, or Tinuvin 384 and the light stabilizer HALS, bis (1, 2, 2, 6, 6-pentamethyl-4-piperidyl) sebacate or Tinuvin 292, were provided by Ciba (Switzerland). The chemical structures of these materials are presented in Figure 1.

The nano-SiO₂ used in this study is non-porous silica (Aerosil 200 F, Antwerp, Belgium). Their average particle size and surface area are 15 nm and 200 m²/g, respectively.

The toluene and butyl acetate solvents which were used were the Chinese P-type.

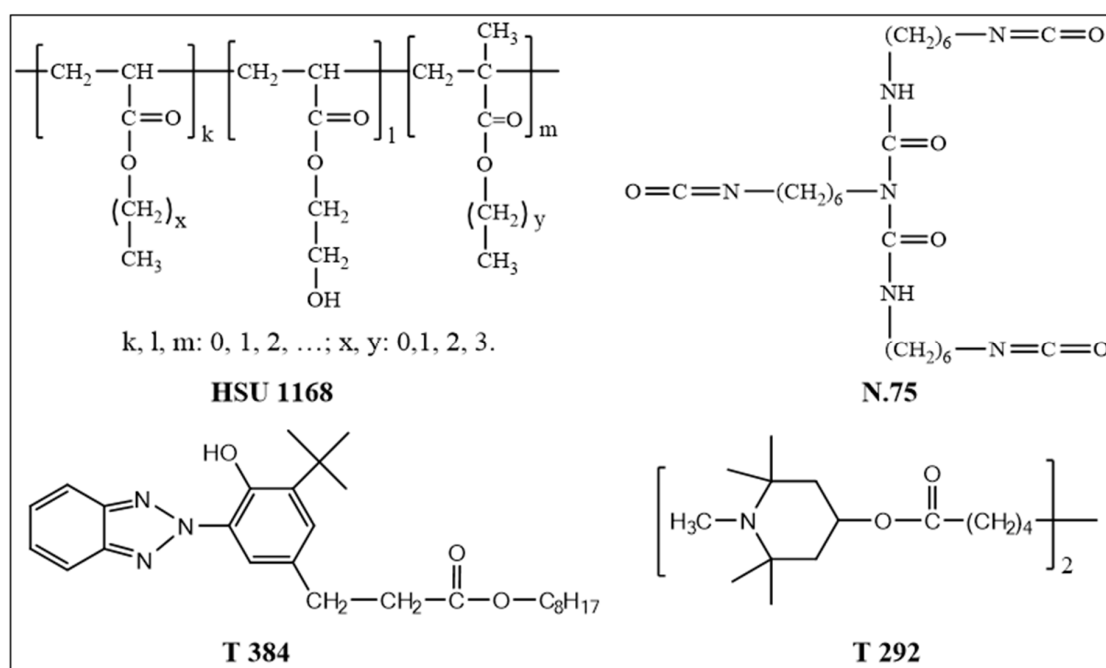


Figure 1. Chemical structures of used compounds.

2.2. Preparation of Coatings

For fabrication of coating, 2 wt % T384, 1 wt % T292, and 2 wt % SiO₂ nanoparticles (by the total solid resin) were selected at the optimal values in our previously published works [5,27]. Weight ratios of materials in coating formulations are presented in Table 1.

At the first step, the nanoparticles were dispersed in the solvent using ultrasonic bath TP 25 for 1 h, then this as-prepared solution was mixed with acrylic polyol resin solution, T384, and T292 by stirring for 15 min. The obtained mixtures were continuously homogenized by ultrasonic bath for 3 h to ensure that the nanoparticles were well dispersed.

The coating samples (with quasi-constant thickness of ~25 µm) were prepared by using a Quadruple Film Applicator (Erichsen model 360, Hemer, Germany). For infrared (IR), ultraviolet-visible (UV-Vis), and field emission scanning electron microscopy (FESEM) analysis, coating samples were prepared on the Teflon sheets, then after 6 days of curing at room temperature separated and attached to aluminum windows. The coating samples for monitoring the weight loss were prepared on glass sheets (100 × 70 × 2 mm) whereas for measuring the gloss and the abrasion resistance, coating samples were prepared on CT3 steel sheets (100 × 100 × 2 mm).

Table 1. Weight ratios of components in coating formulations.

No	Materials	Coating Samples		
		ACPU	ACPU/SiO ₂	ACPU/SiO ₂ -T
1	HSU 1168	60.40	60.40	60.40
2	SiO ₂	0	1.33	1.33
3	T 384	0	0	1.33
4	T 292	0	0	0.66
5	Toluene	18.10	18.76	18.76
6	Butyl acetate	18.10	18.76	18.76
7	N-75	36.20	36.20	36.20

Note: The contents of nano-SiO₂, T 384, and T 292 were 2%, 1.5%, and 1.0% by weight of the total solid resin, respectively.

2.3. Accelerated Weathering Test

The accelerated weathering test was carried out in the Atlas UV/CON chamber (model UC-327-2, Chicago, IL, USA), under UV-A 340 fluorescent lamp, according to ASTM D 4587-05 standard (every testing cycle consists of 8 h for UV exposure at 60 °C and further 4 h for condensate water at 50 °C).

2.4. Characterizations

2.4.1. Field Emission Scanning Electron Microscopy (FESEM) and Transmission Electron Microscopy (TEM) Analysis

The morphology and size of nano-SiO₂ were observed by FESEM S 4800 (Hitachi, Tokyo, Japan) and TEM-JEM 2100 (JEOL, Tokyo, Japan). FE-SEM technique was also used to assess the aging of the coatings under impact of accelerated weathering factors.

2.4.2. Infrared (IR) Analysis

The variations in chemical structures of the coating during the test were monitored by IR spectra on FT-IR spectroscopy (NEXUS 670, Nicolet Instrument Corporation, Madison, WI, USA). The quantitative analysis of the structural groups was calculated based on the changes in optical density of their characteristic absorption by the method we reported previously [3,5,7].

2.4.3. Ultraviolet-Visible (UV-Vis) Analysis

The UV-Vis absorption spectra of the coatings were analyzed on UV-Vis spectrophotometer (GBC, CINTRA 40, Austin, TX, USA) and performed on the samples which were examined by IR analysis.

2.4.4. Weight Loss Measurements

The remaining weight of the coatings was calculated as follows:

$$\text{Remaining weight (\%)} = (m_t/m_0) \times 100 \quad (1)$$

where m_0 and m_t are weights of the coating (dried at 60 °C in vacuum oven until the constant weight) before and after the aging test, respectively.

2.4.5. Gloss Loss Measurements

The gloss of the coatings was measured on the Erichsen Picogloss model 503 equipment at 60° angle. The remaining gloss of the coating was determined by the following expression:

$$\text{Remaining gloss (\%)} = (G_t/G_0) \times 100 \quad (2)$$

where G_0 and G_t are gloss of the coating (dried at 60 °C in vacuum oven until the constant weight) before and after the aging test, respectively.

2.4.6. Determination of Abrasion Resistance

The abrasion resistance of the coatings was determined by falling sand abrasion method according to ASTM D968 standard [27]. The obtained data were the average values from three measurements of each sample.

3. Results and Discussion

3.1. Morphology Study of Coating

Figure 2 presents the FESEM and TEM images of the as-received nano-SiO₂. As can be seen in this figure, the average size of these nanoparticles ranges from 15 to 20 nm. It was a challenge to disperse homogeneously these small nanoparticles in polymer matrix. In this study, a 25 KHz supersonic bath was used to prepare the formulations of the nanocomposite coatings.

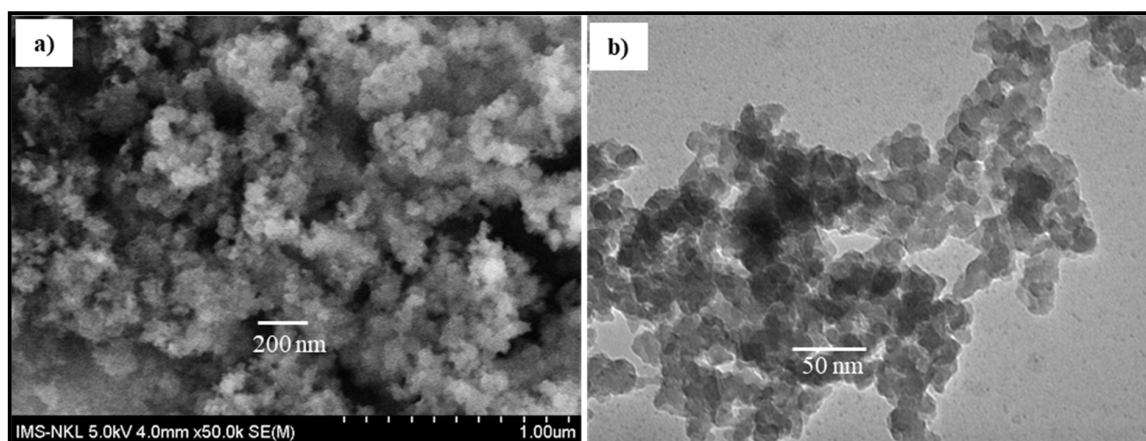


Figure 2. Field emission scanning electron microscopy (FESEM) (a) and transmission electron microscopy (TEM) (b) images of used SiO₂ nanoparticles.

Figure 3 presents the FESEM images of the neat coating (0% nano-SiO₂), nanocomposite coating without organic photostabilizers (2 wt % nano-SiO₂), nanocomposite coating with the photostabilizers (2 wt % nano-SiO₂, 2 wt % T384, and 1 wt % T292), before and after 36 aging cycles.

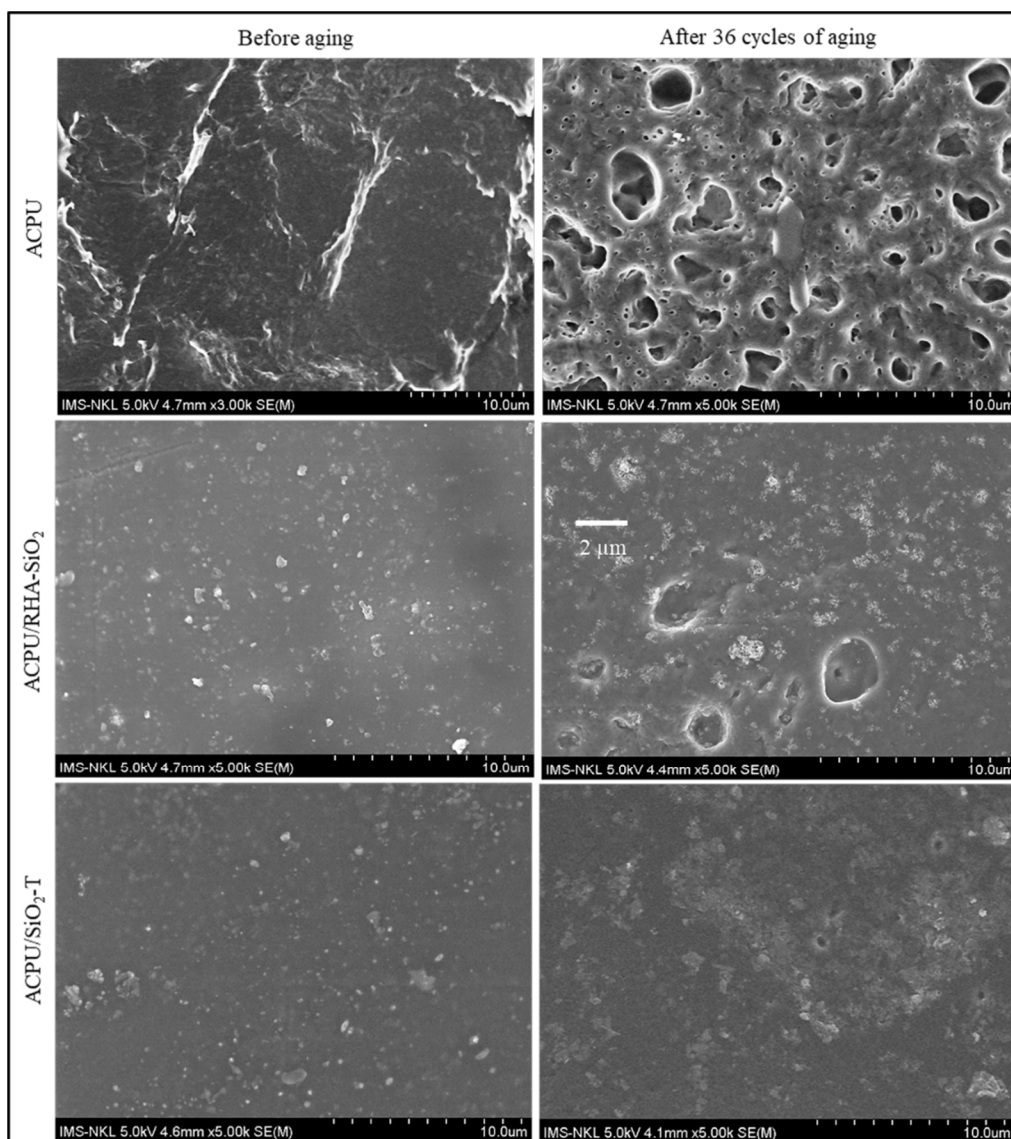


Figure 3. FESEM images of the coatings before (left) and 36 cycles of aging (right).

Before aging test, as shown in Figure 3, nanoparticles were dispersed evenly inside the coatings, providing a tight structure. Thus, incorporation of nano-SiO₂ in polymer matrix should enhance the abrasion resistance of coating [27]. Besides, the light stabilizer, as viscous liquid—plasticizer [3]—might cause the softening effect to the coating. Thus, the abrasion resistance of coating containing stabilizer should decrease as compared to that of the one without stabilizer.

After 36 testing cycles (right side on Figure 3), the neat coating was destroyed seriously with the presence of many pits and pores (ranging in size from 100 nm to μm) appearing on both surface and inside the coating. Whereas, by the presence of 2 wt % nano-SiO₂, only few pits (size of a few micrometers) could be observed on the nanocomposite surface. The size of these pits was reduced (up to a few hundred nanometers) when 2 wt % T 384 and 1 wt % T 292 were added into the coating formulation.

3.2. IR Spectra Study

The changes in chemical structures of coatings (under weathering test) can be evaluated by using IR spectra measurement. Under impacts of the weathering factors, chemical bonds in the polymer chain can be broken, leading to the loss of bonds or the formation of new bonds. Therefore, the investigation of these chemical variations can clarify the degradation mechanism of organic coatings during the

aging process. In this study, the variations in chemical structures of the coatings were evaluated by IR method. The IR spectra of the coatings before and after 36 testing cycles are presented in the Figure 4. Figure 5 presents the changes of alkane CH groups and CNH groups in the coating samples, which were deduced from the quantitative IR spectra analysis. Three coating samples were tested, such as (i) neat coating (ACPU), (ii) nanocomposite coating with 2 wt % nano-SiO₂ (ACPU/SiO₂), (iii) nanocomposite coating with 2 wt % SiO₂, 2 wt % T384, and 1 wt % T292. In addition, as the reference, we added the changes of alkane CH groups and CNH groups in the coating contained only 2 organic stabilizers (i.e., 2 wt % T384 and 1 wt % T292 -ACPU-T) [3], shown in Figure 5.

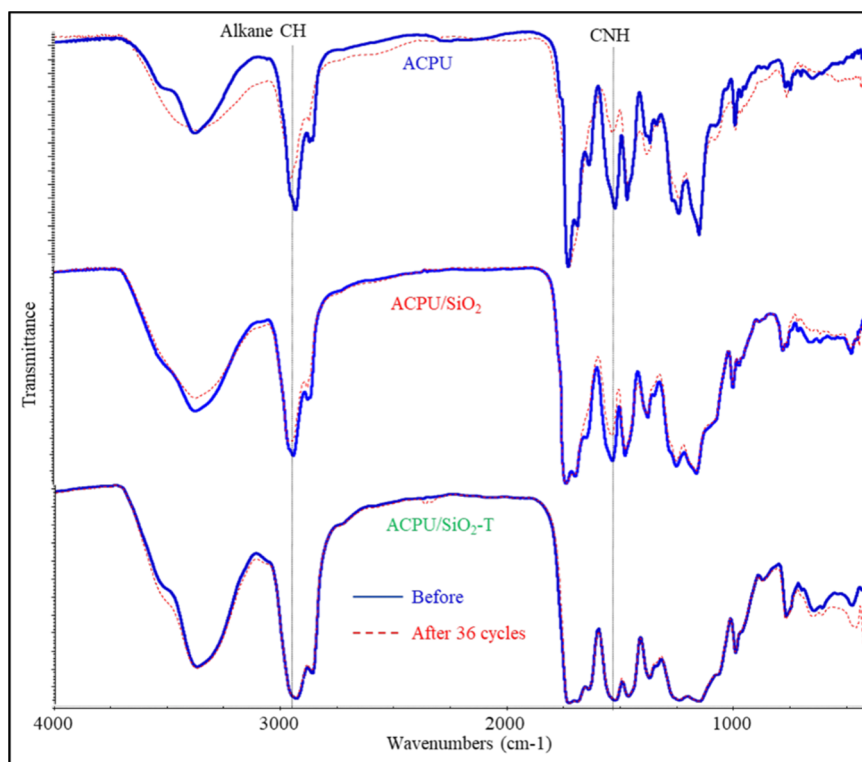


Figure 4. Infrared (IR) spectra of neat coating (ACPU), nanocomposite coating containing 2 wt % nano-SiO₂ (ACPU/SiO₂), and nanocomposite coating containing 2 wt % nano-SiO₂, 2 wt % T 384, and 1 wt % T 292 (ACPU/SiO₂-T), before and after 36 aging cycles.

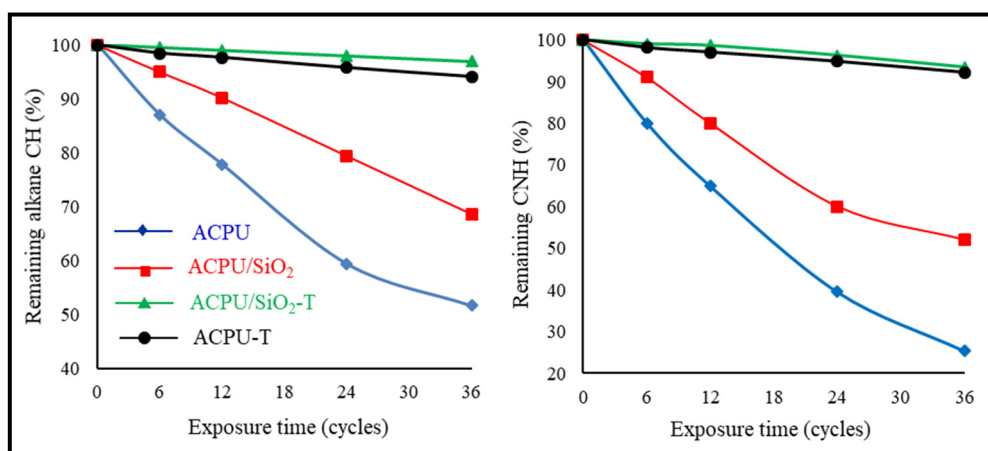


Figure 5. Chemical changes of the alkane CH (left) and CNH (right) groups in the various coatings under accelerated weathering condition.

As can be seen in Figures 4 and 5, during the testing process, the peaks at 2950 and 1527 cm^{-1} characterizing the alkane CH groups and CNH groups in the coatings both decreased. Their intensity reduced the most strongly in the neat coating, but least in the coating containing the nanoparticles and organic light stabilizers. After 36 testing cycles, the remaining content of alkane CH groups were 51.6%, 68.6%, and 97.1%, in the neat coating (ACPU), the nanocomposite coating with 2 wt % nano-SiO₂ (ACPU/SiO₂), and the nanocomposite coating with 2 wt % nano-SiO₂, 2 wt % T384, and 1 wt % T292 (ACPU/SiO₂-T), respectively. In the case of CNH groups, their remaining content was 25.4%, 52.1%, 93.5% in ACPU, ACPU/SiO₂, and ACPU/SiO₂-T coatings, respectively.

For comparative study, the chemical changes in the ACPU/SiO₂-T coating were lower than that in the ACPU-T coating.

3.3. Weight Loss Study

The variations in weight of the ACPU, ACPU/SiO₂, and ACPU/SiO₂-T coatings during the aging test are shown in Figure 6. Besides, as the reference, we added the weight changes of ACPU-T coating [3] into Figure 6.

As shown in Figure 6, the weight loss of all coatings increased by testing time. It reached the highest value for the neat coating and the coating containing light stabilizer had the smallest value of weight loss. Quantitatively, after 36 cycles, the remaining weights of the ACPU, ACPU/SiO₂, and ACPU/SiO₂-T coatings were 87.26%, 90.26%, and 97.8%, respectively. For comparative study, the weight loss in ACPU/SiO₂-T coating was lower than that in ACPU-T coating.

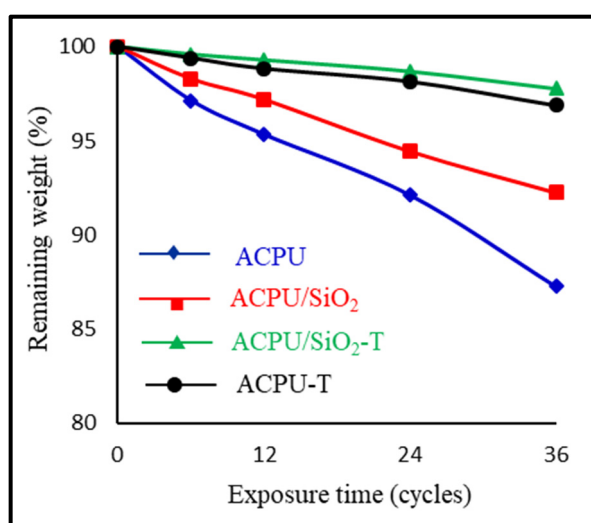


Figure 6. Changes in weight of the coatings under accelerated weathering aging condition.

3.4. Coating Gloss Loss Study

The weathering aging causes the degradation in properties of the coating. Hence, the degradation of the coating under the weathering factors can be evaluated by monitoring the variations in their properties. Figure 7 demonstrates the variations in gloss of the ACPU, ACPU/SiO₂, and ACPU/SiO₂-T coatings during aging process. Besides, as the reference, we added the gloss changes of ACPU-T coating [3] into Figure 7.

From Figure 7, it can be seen that the gloss of the coatings decreased by aging time. The gloss of the neat coating was lost significantly. The gloss of the nanocomposite coating containing light stabilizer, by contrast, was lost slightly. After 36 aging cycles, the gloss value of the ACPU, ACPU/SiO₂, and ACPU/SiO₂-T coatings, remained at 83.3%, 92.5%, and 98.5%, respectively. For comparative study, the gloss change in ACPU/SiO₂-T coating was lower than that in ACPU-T coating.

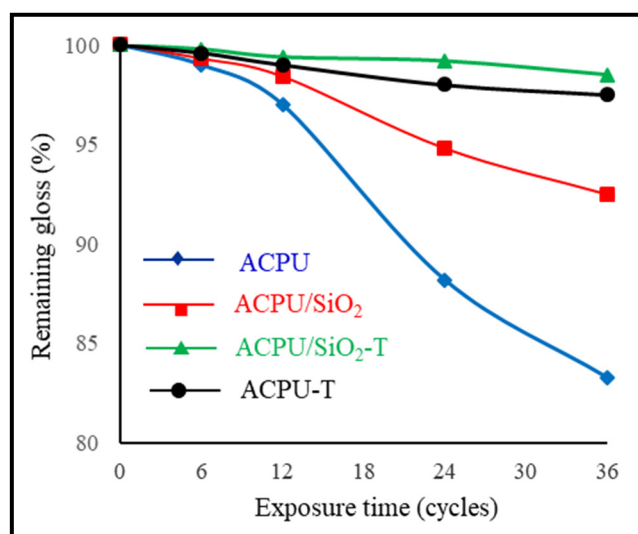


Figure 7. Changes in gloss of the coatings under accelerated weathering aging condition.

3.5. Coating Abrasion Study

Figure 8 presents the abrasion resistance of the ACPUs, ACPUsiO₂, and ACPUsiO₂-T coatings, before and after 36 aging cycles.

As seen in Figure 8, adding 2 wt % nano-SiO₂ to the paint formulation increased significantly the abrasion resistance of coating from 130 to 240 lite/mil. When added 2 wt % T 384 and 1 wt % T 292, the abrasion resistance of coating slightly decreased from 240 to 235 lite/mil. After 36 aging cycles, the abrasion resistance of the neat coating reduced strongly (down to 38.46%), from 130 to 80 lite/mil. However, the abrasion resistance of coating containing 2 wt % nano-SiO₂ reduced slightly from 240 to 220 lite/mil (8.33%). Whereas in the case of ACPUsiO₂-T coating, reduction was only 2.12% (235 to 230 lite/mil) after aging test.

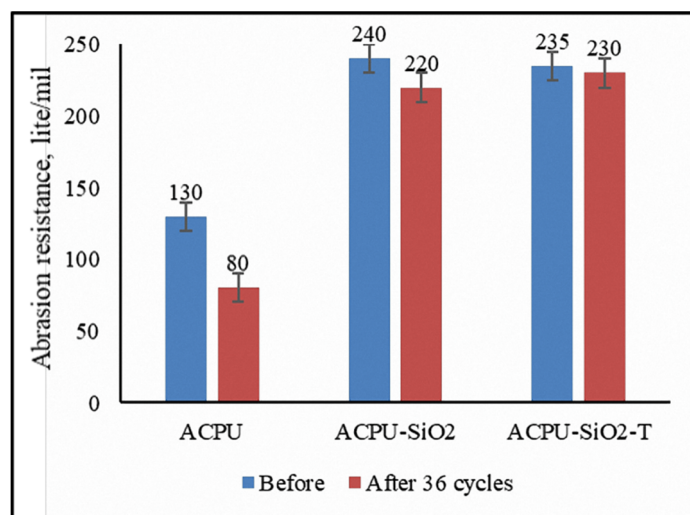


Figure 8. Values of abrasion resistance for coatings, before and after 36 cycles of aging.

As can be seen in Figure 8, addition of nano-SiO₂, UV absorber T384, and light stabilizer HALS T292 into coating matrix significantly improved the weathering durability of the coating. As a complement data, Figure 9 presents the UV-Vis spectra of aqueous solution containing nano-SiO₂ (0.5 wt % dispersion), ACPUs, ACPUsiO₂, and ACPUsiO₂-T coatings.

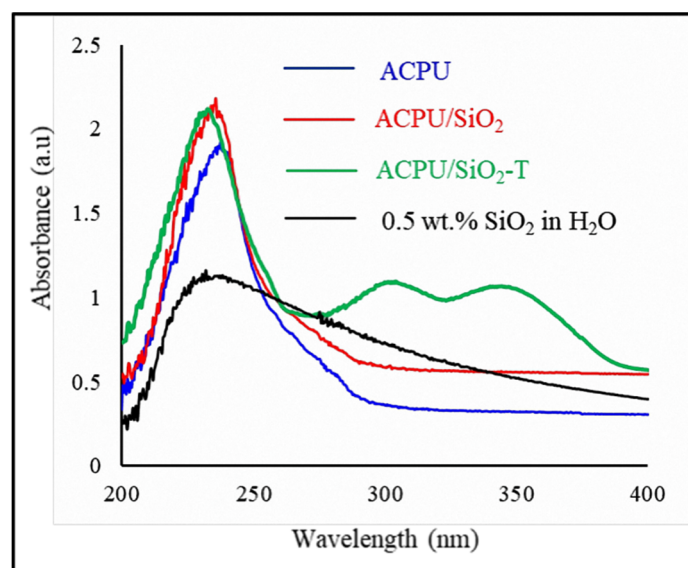


Figure 9. Ultraviolet-visible (UV-Vis) spectra of the various coating samples and the aqueous solution of nano-SiO₂.

As shown in Figure 9, the absorption of UV radiation was much lower (less effective) for the ACPU coating, as compared to the ACPU/SiO₂-T coating. In particular, the UV absorption of ACPU/SiO₂-T coating was the strongest among these coating samples. As expected, due to the UV absorption of nano-SiO₂, the polymer coating was protected under UV irradiation. Thus, the nanocomposite coating containing 2 wt % SiO₂ exhibited a smaller value in chemical change, leading lower loss in weight, higher gloss, and better abrasion resistance than that of the ACPU coating.

These findings are consistent with the data reported by Yari et al. [18] for the photo-protective effect of nano-SiO₂ on acrylic melamine coating. Moreover, nano-SiO₂ could also react with isocyanate groups [28] to form a tight organic-inorganic hybrid structure, which contributes to preventing the invasion of external environmental factors [29], leading the coating to reduce its degradation effectively. By the presence of 2 wt % T 384 and 1 wt % T 292, the polymer coating is double-protected by the combination of T 384 (as UV absorber) and T 292 (as free radical cleaner). In our previous paper [3], we discussed their photo-protection mechanism. Consequently, ACPU/SiO₂-T coating exhibited an excellent weathering resistance after 36 testing cycles.

The obtained data indicate that incorporation of nanoparticles into the acrylic polyurethane coating (with the presence of photostabilizers) enhances its weathering resistance.

4. Conclusions

The synergistic effects of nano-SiO₂ and organic light stabilizers on enhancing the weathering resistance of acrylic polyurethane coating have been investigated and discussed.

The main findings of this study are:

- The obtained data indicated that incorporation of nano-SiO₂ in the acrylic polyurethane matrix not only improved its mechanical property but also enhanced its weathering resistance.
- After 36 testing cycles, the remaining content of alkane CH groups was 51.6%, 68.6%, and 97.1%, in the ACPU, ACPU/SiO₂, and ACPU/SiO₂-T coatings, respectively. In case of CNH groups, their remained content was 25.4%, 52.1%, 93.5% in the ACPU, ACPU/SiO₂, and ACPU/SiO₂-T coatings, respectively.
- After 36 aging cycles, the gloss remaining values of ACPU, ACPU/SiO₂, and ACPU/SiO₂-T coatings, were 83.3%, 92.5%, and 98.5 %, respectively.
- After 36 aging cycles, the abrasion resistance of the ACPU coating reduced strongly (down to 38.46%), from 130 to 80 lite/mil. However, for ACPU/SiO₂ coating, it reduced slightly from 240 to

220 lite/mil (8.33%). In the case of ACPU/SiO₂-T coating its reduction was only 2.12% (from 235 to 230 lite/mil) after aging test.

These enhancements could be explained by two possible reasons: (i) UV absorption of nanofillers (nano-SiO₂), could photo-protect the polymer coating, and (ii) a tight organic-inorganic hybrid structure was formed under curing reactions. Besides, addition of organic light stabilizer into paint formulation has provided excellent weathering resistance for the nanocomposite coating. These findings indicated the promising application of this nanocomposite coating as a multi-functional durable material.

Author Contributions: Conceptualization and writing—the original draft: T.V.N.; Experimentals and data analysis: T.H.N.; Writing—review and editing: T.A.N. All authors have read and agreed to the published version of the manuscript.

Funding: This work was financially supported by the Vietnam National Foundation for Science and Technology Development (NAFOSTED, Grant # 104.02-2018.19).

Conflicts of Interest: The authors declare no conflict of interest.

References

1. Nguyen, T.N.L.; Do, T.V.; Nguyen, T.V.; Hung, D.P.; Trinh, V.T.; Mac, V.P.; Nguyen, A.H.; Le, T.L.; Nguyen, T.A.; Vo, T.K.A.; et al. Antimicrobial activity of acrylic polyurethane/Fe₃O₄-Ag nanocomposite coating. *Prog. Org. Coat.* **2019**, *132*, 15–20. [\[CrossRef\]](#)
2. Maganty, S.; Roma, M.P.C.; Meschter, S.J.; Starkey, D.; Gomez, M.; Edwards, D.G.; Elskens, A.E.K.; Cho, J. Enhanced mechanical properties of polyurethane composite coatings through nanosilica addition. *Prog. Org. Coat.* **2016**, *90*, 243–251. [\[CrossRef\]](#)
3. Nguyen, T.V.; Le, X.H.; Dao, P.H.; Decker, C.; Nguyen, T.P. Stability of acrylic polyurethane coatings under accelerated aging tests and natural outdoor exposure: The critical role of the used photo-stabilizers. *Prog. Org. Coat.* **2018**, *124*, 137–146. [\[CrossRef\]](#)
4. Chen, X.D.; Wang, Z.; Liao, Z.F.; Mai, Y.L.; Zhang, M.Q. Roles of anatase and rutile TiO₂ nanoparticles in photooxidation of polyurethane. *Polym. Test.* **2007**, *26*, 202–208. [\[CrossRef\]](#)
5. Nguyen, T.V.; Nguyen, T.P.; Nguyen, T.D.; Aidani, R.; Trinh, V.T.; Decker, C. Accelerated degradation of water borne acrylic nanocomposites used outdoor protective coatings. *Polym. Degrad. Stab.* **2016**, *128*, 65–76. [\[CrossRef\]](#)
6. Nguyen, T.V.; Dao, P.H.; Duong, K.L.; Duong, Q.H.; Vu, Q.T.; Nguyen, A.H.; Mac, V.P.; Le, T.L. Effect of R-TiO₂ and ZnO nanoparticles on the UV-shielding efficiency of water-borne acrylic coating. *Prog. Org. Coat.* **2017**, *110*, 114–121. [\[CrossRef\]](#)
7. Nguyen, T.V.; Nguyen, T.A.; Dao, P.H.; Mac, V.P.; Nguyen, A.H.; Do, M.T.; Nguyen, T.H. Effect of rutile titania dioxide nanoparticles on the mechanical property, thermal stability, weathering resistance and antibacterial property of styrene acrylic polyurethane coating. *Adv. Nat. Sci. Nanosci. Nanotechnol.* **2016**, *7*, 045015–045024. [\[CrossRef\]](#)
8. Seentrakoon, B.; Junhasavasdikul, B.; Chavasiri, W. Enhanced UV-protection and antibacterial properties of natural rubber/rutile-TiO₂ nanocomposites. *Polym. Degrad. Stab.* **2013**, *98*, 566–578. [\[CrossRef\]](#)
9. Nguyen, T.V.; Tri, P.N.; Azizi, S.; Dang, T.C.; Hoang, D.M.; Hoang, T.H.; Nguyen, T.L.; Bui, T.T.L.; Dang, V.H.; Nguyen, N.L.; et al. The role of organic and inorganic UV-absorbents on photopolymerization and mechanical properties of acrylate-urethane coating. *J. Mater. Today Commun.* **2020**, *22*, 100780. [\[CrossRef\]](#)
10. Tri, P.N.; Nguyen, T.A.; Nguyen, T.H.; Carriere, P. Antibacterial behavior of hybrid nanoparticles—Chapter 7. In *Noble Metal-Metal Oxide Hybrid Nanoparticles: Fundamentals and Applications*; Mohapatra, S., Nguyen, T.A., Nguyen-Tri, P., Eds.; Elsevier: Amsterdam, The Netherlands, 2019; pp. 141–155. [\[CrossRef\]](#)
11. Ngo, T.D.; Le, T.M.H.; Nguyen, T.H.; Nguyen, T.V.; Nguyen, T.A.; Le, T.L.; Nguyen, T.T.; Tran, T.T.V.; Le, T.B.T. Antibacterial nanocomposites based on Fe₃O₄-Ag hybrid nanoparticles and natural rubber-polyethylene blends. *Int. J. Polym. Sci.* **2016**, *2016*. [\[CrossRef\]](#)
12. Nguyen, T.V.; Do, T.V.; Ha, M.H.; Le, H.K.; Le, T.T.; Nguyen, T.N.L.; Dam, X.T.; Lu, L.T.; Tran, D.L.; Vu, Q.T.; et al. Crosslinking process, mechanical and antibacterial properties of UV-curable acrylate/Fe₃O₄-Ag nanocomposite coating. *J. Prog. Org. Coat.* **2020**, *139*, 105325. [\[CrossRef\]](#)

13. Nguyen, T.H.; Nguyen, T.A.; Nguyen, T.V.; Le, V.K.; Dinh, T.M.T.; Thai, H.; Shi, X. Effect of Electrochemical Injection of Corrosion Inhibitor (EICI) on the corrosion of steel rebar in chloride contaminated mortar. *Int. J. Corros.* **2015**, *2015*. [\[CrossRef\]](#)
14. Nguyen, T.V.; Dao, P.H.; Nguyen, T.A.; Dang, V.H.; Ha, M.N.; Nguyen, T.T.T.; Vu, Q.T.; Nguyen, N.L.; Dang, C.T.; Tri, P.N.; et al. Photocatalytic degradation and heat reflectance recovery of water-borne acrylic polymer/ZnO nanocomposite coating. *J. Compos. Sci.* **2020**. [\[CrossRef\]](#)
15. Wu, G.; Liu, D.; Chen, J.; Liu, G.; Kong, Z. Preparation and properties of super hydrophobic films from siloxane-modified two-component waterborne polyurethane and hydrophobic nano SiO₂. *Prog. Org. Coat.* **2019**, *127*, 80–87. [\[CrossRef\]](#)
16. Jouyandeh, M.; Rahmati, N.; Movahedifar, E.; Hadavand, B.S.; Karami, Z.; Ghaffari, M.; Taheri, P.; Bakhshandeh, E.; Vahabi, H.; Ganjali, M.R.; et al. Properties of nano-Fe₃O₄ incorporated epoxy coatings from cure index perspective. *Prog. Org. Coat.* **2019**, *133*, 220–228. [\[CrossRef\]](#)
17. Allahverdi, A.; Ehsani, M.; Janpour, H.; Ahmadi, S. The effect of nanosilica on mechanical, thermal and morphological properties of epoxy coating. *Prog. Org. Coat.* **2012**, *75*, 543–548. [\[CrossRef\]](#)
18. Yari, H.; Moradian, S.; Tahmasebi, N. The weathering performance of acrylic melamine automotive clearcoats containing hydrophobic nanosilica. *J. Coat. Technol. Res.* **2013**, *11*, 351–360. [\[CrossRef\]](#)
19. Dao, P.H.; Nguyen, T.V.; Dang, M.H.; Nguyen, T.L.; Trinh, V.T.; Mac, V.P.; Nguyen, A.H.; Duong, T.M. Effect of silica nanoparticles on properties of coatings based on acrylic emulsion resin. *Vietnam J. Sci. Technol.* **2018**, *56*, 117–125.
20. Nguyen, T.A.; Nguyen, T.H.; Nguyen, T.V.; Thai, H.; Shi, X. Effect of nanoparticles on the thermal and mechanical properties of epoxy coatings. *J. Nanosci. Nanotechnol.* **2016**, *16*, 9874–9881. [\[CrossRef\]](#)
21. Shi, X.; Nguyen, T.A.; Suo, Z.; Liu, Y.; Avci, R. Effect of nanoparticles on the anticorrosion and mechanical properties of epoxy coating. *Surf. Coat. Technol.* **2009**, *204*, 237–245. [\[CrossRef\]](#)
22. Junaidi, M.U.M.; Azaman, S.A.H.; Ahmad, N.N.R.; Leo, C.P.; Lim, G.W.; Chan, D.J.C.; Yee, H.M. Superhydrophobic coating of silica with photoluminescence properties synthesized from rice husk ash. *Prog. Org. Coat.* **2017**, *111*, 29–37. [\[CrossRef\]](#)
23. Kumar, A.M.; Latthe, S.S.; Sudhagar, P.; Obot, I.B.; Gasem, Z.M. In-situ synthesis of hydrophobic SiO₂-PMMA composite for surface protective coatings: Experimental and quantum chemical analysis. *Polymer* **2015**, *77*, 79–86. [\[CrossRef\]](#)
24. Ammar, S.; Ramesh, K.; Ma, I.A.W.; Farah, Z.; Arof, A.K. Studies on SiO₂-hybrid polymeric nanocomposite coatings with superior corrosion protection and hydrophobicity. *Surf. Coat. Technol.* **2017**, *324*, 536–545. [\[CrossRef\]](#)
25. Chen, H.; Zhang, X.; Zhang, P.; Zhang, Z. Facile approach in fabricating superhydrophobic SiO₂/polymer nanocomposite coating. *Appl. Surf. Sci.* **2012**, *261*, 628–632. [\[CrossRef\]](#)
26. Lin, B.; Zhou, S. Poly(ethylene glycol)-grafted silica nanoparticles for highly hydrophilic acrylic-based polyurethane coatings. *Prog. Org. Coat.* **2017**, *106*, 145–154. [\[CrossRef\]](#)
27. Le, T.T.; Nguyen, T.V.; Nguyen, T.A.; Nguyen, T.H.; Hoang, T.; Tran, D.L.; Dinh, D.A.; Nguyen, T.M.; Lu, T. Thermal, mechanical and antibacterial properties of water-based acrylic polymer/SiO₂-Ag nanocomposite coating. *J. Mater. Chem. Phys.* **2019**, *232*, 362–366. [\[CrossRef\]](#)
28. Mekuria, T.D.; Zhang, C.; Liu, Y.; Diao, E.D.F.; Zhou, Y. Surface modification of nano-silica by diisocyanates and their application in polyimide matrix for enhanced mechanical, thermal and water proof properties. *Mater. Chem. Phys.* **2019**, *225*, 358–364. [\[CrossRef\]](#)
29. Bui, T.M.A.; Nguyen, T.V.; Nguyen, T.M.; Hoang, H.; Nguyen, T.T.; Lai, T.H.; Tran, T.N.; Nguyen, V.H.; Hoang, V.H.; Le, T.L.; et al. Investigation of crosslinking, mechanical properties and weathering stability of acrylic polyurethane nanocomposite coating reinforced by SiO₂ nanoparticles issued from rice husk ash. *J. Mater. Chem. Phys.* **2020**, *241*, 122445. [\[CrossRef\]](#)

